Cell Reports

Report

H4K44 Acetylation Facilitates Chromatin Accessibility during Meiosis

Graphical Abstract

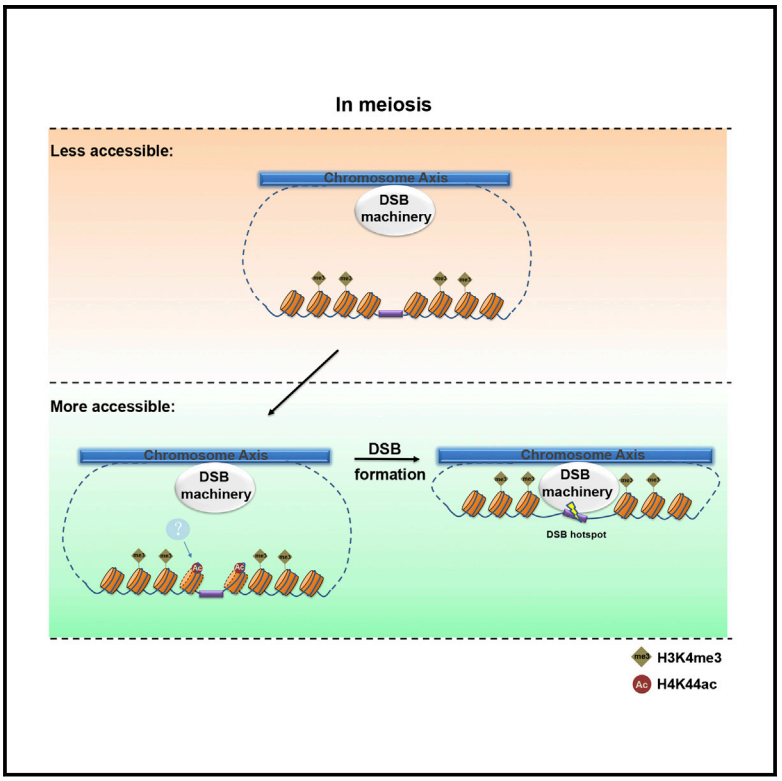

Authors

Jialei Hu, Greg Donahue, Jean Dorsey, ..., Benjamin A. Garcia, Parisha P. Shah, Shelley L. Berger

Correspondence

parisha@mail.med.upenn.edu (P.P.S.), bergers@upenn.edu (S.L.B.)

In Brief

Hu et al. find that H4K44 is acetylated in sporulating yeast and that this modification is required for meiotic recombination, as well as being associated with meiotic DSB hotpots genome-wide.

Highlights

- H4K44 is acetylated in sporulating cells but not in vegetative cells
- H4K44ac is required for normal meiotic recombination
- H4K44ac is associated with meiotic DSB hotspots genome-wide
- H4K44ac confers chromatin accessibility at DSB hotspots

Accession Numbers

GSE59005

Hu et al., 2015, Cell Reports *13*, 1772–1780
December 1, 2015 ©2015 The Authors
http://dx.doi.org/10.1016/j.celrep.2015.10.070

CellPress

OPEN ACCESS
CellPress

Cell Reports
Report

H4K44 Acetylation Facilitates Chromatin Accessibility during Meiosis

Jialei Hu,[1,2] Greg Donahue,[1,2] Jean Dorsey,[1,2] Jérôme Govin,[1,4] Zuofei Yuan,[2,3] Benjamin A. Garcia,[2,3] Parisha P. Shah,[1,2,*] and Shelley L. Berger[1,2,*]
[1]Department of Cell and Developmental Biology
[2]Epigenetics Program
University of Pennsylvania, Philadelphia, PA 19104, USA
[3]Department of Biochemistry and Biophysics, Epigenetics Program, University of Pennsylvania, Philadelphia, PA 19104, USA
[4]Laboratoire Biologie à Grande Echelle, INSERM, U1038 Grenoble, France
*Correspondence: parisha@mail.med.upenn.edu (P.P.S.), bergers@upenn.edu (S.L.B.)
http://dx.doi.org/10.1016/j.celrep.2015.10.070

SUMMARY

Meiotic recombination hotspots are associated with histone post-translational modifications and open chromatin. However, it remains unclear how histone modifications and chromatin structure regulate meiotic recombination. Here, we identify acetylation of histone H4 at Lys44 (H4K44ac) occurring on the nucleosomal lateral surface. We show that H4K44 is acetylated at pre-meiosis and meiosis and displays genome-wide enrichment at recombination hotspots in meiosis. Acetylation at H4K44 is required for normal meiotic recombination, normal levels of double-strand breaks (DSBs) during meiosis, and optimal sporulation. Non-modifiable H4K44R results in increased nucleosomal occupancy around DSB hotspots. Our results indicate that H4K44ac functions to facilitate chromatin accessibility favorable for normal DSB formation and meiotic recombination.

INTRODUCTION

Modulating accessibility of the nucleosomal DNA is critical for transcription, replication, recombination, and DNA damage repair (Bell et al., 2011). In these processes, histone modifications are key players, functioning either as docking sites for recruiting *trans*-acting proteins or to directly influence the chromatin structure, thus affecting DNA accessibility. In their *trans*-acting role, histone modifications commonly recruit effectors to influence chromatin function via association with specialized protein domains, such as PHD domains (Wysocka et al., 2006) or bromodomains (Musselman et al., 2012). In contrast, modifications on the histone globular cores directly modulate chromatin structure. For example, lysine acetylation on the nucleosome lateral surface, including H3K56, H3K64, H3K115, H3K122, H4K77, and H4K79, can regulate DNA accessibility by facilitating nucleosome mobility or histone eviction (Tropberger and Schneider, 2013). These findings support a model whereby lateral surface modifications alter nucleosome mobility and stability (Cosgrove et al., 2004).

An important biological function regulated by DNA accessibility is meiotic homologous recombination. In most sexual species, meiotic recombination ensures accurate chromosome segregation and generates genetic diversity in gametes. Meiotic recombination is triggered by the formation of programmed DNA double-strand breaks (DSBs), catalyzed by the conserved topoisomerase-related Spo11 (Keeney, 2001). In *S. cerevisiae*, at least nine additional factors are required for DSB formation (Keeney, 2008). After DSB formation, Rad51 and Dmc1 recombinases are involved in the repair of meiotic DSBs (Hunter, 2007).

Multiple chromatin features are associated with meiotic recombination in *S. cerevisiae*. Meiotic recombination occurs preferentially at specific sites (hotspots), which often reside in open regions at most gene promoters (Pan et al., 2011); the open configuration is believed to contribute to initiation of recombination (Wu and Lichten, 1994). Some hotspots exhibit increased nuclease sensitivity shortly before DSB formation (Ohta et al., 1994), indicative of active chromatin remodeling to increase DNA accessibility. DSB hotspots are also enriched for specific histone modifications (Zhang et al., 2011), including H3K4me3, which may be a major determinant of DSB location (Borde et al., 2009; Sollier et al., 2004). The mechanistic link between histone methylation and DSB formation is achieved by the complex proteins associated with Set1 subunit Spp1 (Acquaviva et al., 2013; Sommermeyer et al., 2013); however, it remains unclear how chromatin structure is regulated to favor DSB formation.

In a previous study, we carried out a mutational screen of modifiable residues on histones H3 and H4 to uncover substitutions that affect sporulation efficiency in *S. cerevisiae* (Govin et al., 2010a). A number of modifications were located on the nucleosome lateral surface, indicating an important function for chromatin structure regulation. Here, we describe an acetylation site on Lys44 on histone H4 (H4K44ac) on the nucleosome lateral surface. We show that H4K44ac is associated with meiotic recombination, and our results suggest an important role for H4K44ac in promoting an accessible chromatin environment for efficient programmed DNA recombination.

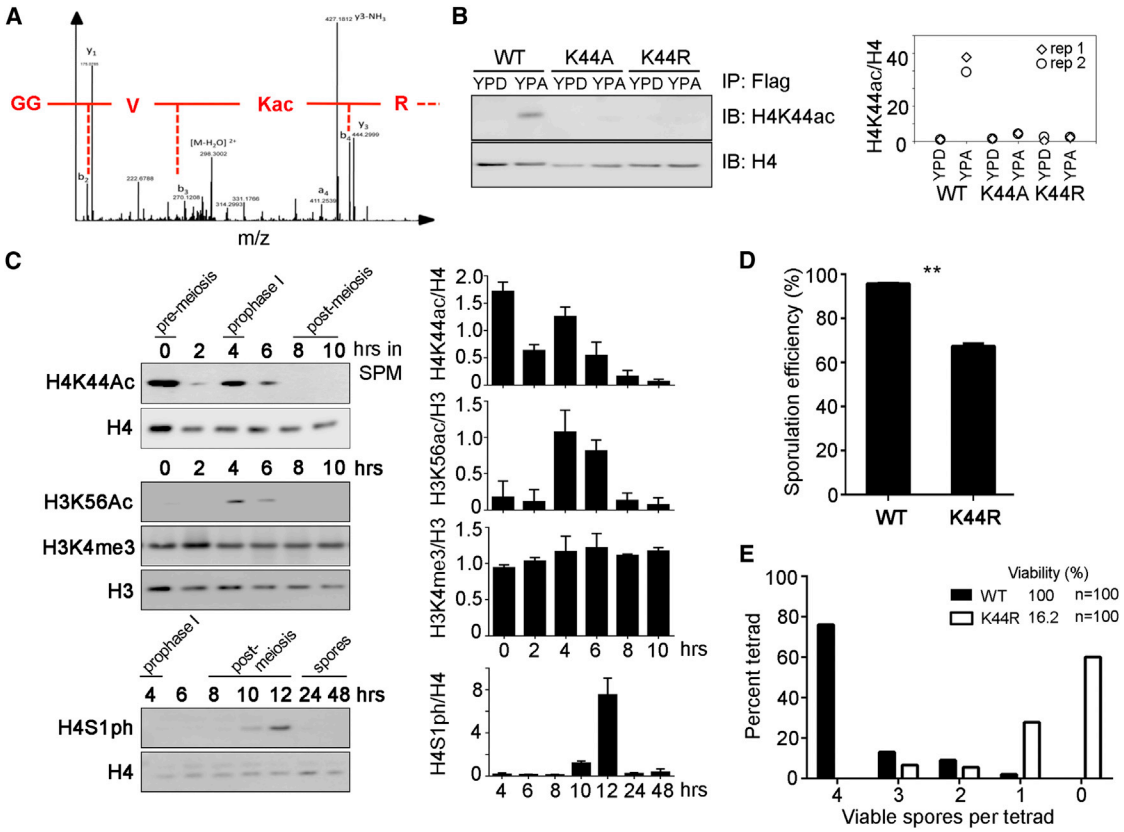

Figure 1. Histone H4K44 Is Acetylated in Sporulation and Is Important for Normal Sporulation Efficiency

(A) Mass spectrometry analysis of histones during sporulation. Fragmentation of the parent ion (histone H4 41-GGVK$_{ac}$R-45) with m/z = 307.688. The arrows bracket the peaks that define the presence of acetyl-lysine (Kac).

(B) Representative western blot (left) of FLAG-tagged histone H4 immunoprecipitated with FLAG antibody from WT and H4K44 mutants probed with antibodies against H4K44ac (top) or total H4 (bottom). H4K44ac is detectable in WT after cells are transferred into acetate (pre-sporulation) medium; H4K44ac is not detectable in H4K44A or H4K44R mutants. Quantification (right) was performed using two biological replicates.

(C) Presence of pre-sporulation H4K44ac, followed by peak of H4K44ac during meiosis (4 hr) and then loss of H4K44ac. Representative western blot (left) for each histone modification throughout sporulation; quantification of each modification (right; mean ± SEM of three independent experiments). SPM, sporulation media.

(D) H4K44 mutants, which have reduced sporulation efficiency as measured by the percentage of tetrads from an initial population of cells induced to sporulation (mean ± SEM of three independent experiments). The difference is statistically significant: **p < 0.01.

(E) H4K44R spores, which are mostly inviable. Four-spore tetrads from three different yeast isolates were dissected for WT and H4K44R strains; distribution of spore viabilities was plotted per tetrad for each strain. n = 100.

See also Figure S1.

RESULTS

H4K44ac Is Important for Yeast Sporulation

We previously identified several modifiable residues on histones H3 and H4 required for yeast sporulation, including residues that reside on the nucleosome globular core (Govin et al., 2010a). To determine which of these residues are modified in meiosis, we purified histones from *S. cerevisiae* meiotic cells and subjected them to chemical derivization via propionylation and nano-liquid chromatography-tandem mass spectrometry analyses. Tandem mass spectrometry revealed a small peptide from the histone H4 core that was acetylated at K44 ($_{pr}$GGVK$_{ac}$R) (Figure 1A). Accurate mass (307.688 m/z) matched the calculated mass of this peptide as acetylated (307.685 m/z), as opposed to tri-methylated (307.703 m/z), and retention time indicated an acetylated rather than a tri-methylated peptide (Figure S1A).

To characterize the H4K44ac modification, we raised an antibody against a synthetic peptide containing acetylated H4K44. Antibody specificity was measured by western blot and dot blot analyses (Figures 1B and S1B). Using this antibody, we observed enrichment of H4K44ac during growth in the pre-sporulation medium and at prophase I in meiosis (Figures 1C and S1C). This pattern is unique compared to other meiosis-associated histone modifications, such as H4S1ph that increases following meiosis or H3K4me3 that is constant through sporulation (Figure 1C) (Govin et al., 2010a; Krishnamoorthy et al., 2006).

To characterize the function of H4K44ac during sporulation, we engineered H4K44 mutant strains harboring non-modifiable H4K44R. Wild-type (WT) and H4K44R strains were sporulated, and cells were collected throughout sporulation to determine the overall sporulation frequency. H4K44R sporulation was significantly lower than WT (63% of WT) (Figure 1D). Most of

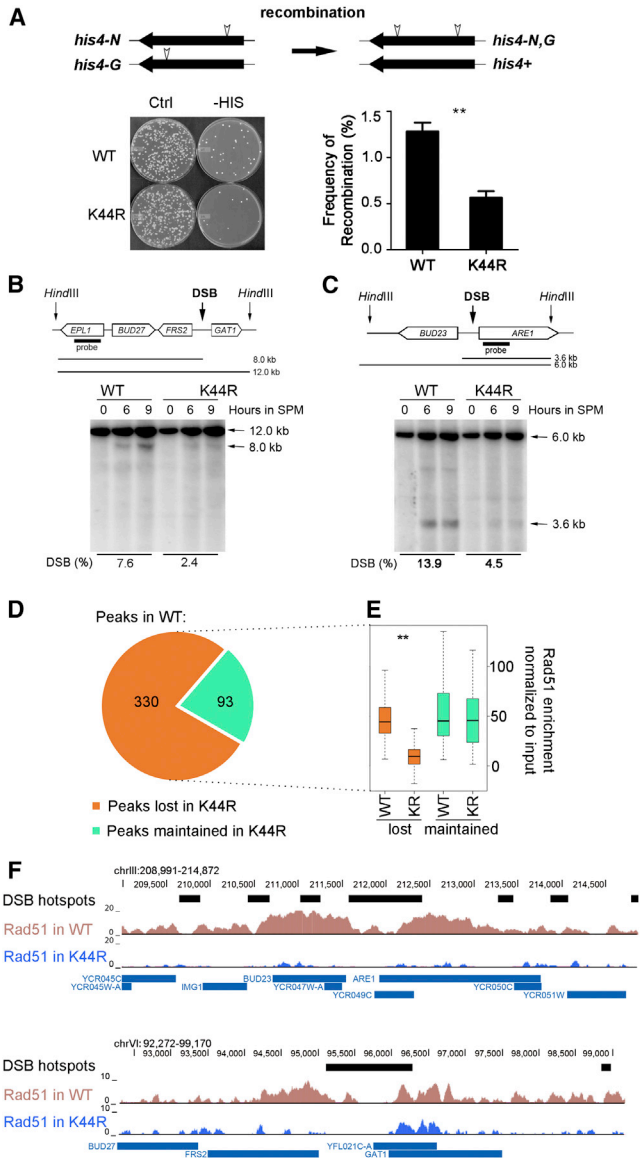

Figure 2. H4K44ac Facilitates Meiotic Recombination

(A) Top: Schematic diagram of intragenic recombination at *his4G* and *his4R* heteroalleles. Bottom left: Random spore analysis from WT and H4K44R strains. Spores were plated on control YPD plates (left) and −HIS selection plates (right); ten times as many spores were plated on −HIS. H4K44R shows reduced recombination compared to WT. Bottom right: Intragenic recombination was calculated as the percentage of HIS+ colonies relative to total viable colonies on the YPD plate (mean ± SEM of three independent experiments). The difference is statistically significant: $^{**}p < 0.01$.

(B and C) H4K44R strains exhibiting fewer DSBs than WT (*sae2Δ* background). Top: Schematic map of the *FRS2-GAT1* (left) and *BUD23-ARE1* (right) loci. The positions of the *Hind*III restriction sites and the sizes of the DSB fragments are indicated; probe locations are marked by the black bars. Bottom: Representative Southern blot for DSB formation across a meiotic time course in WT and H4K44R. n = 3. Arrows indicate the *Hind*III fragment without DSBs and fragments corresponding to meiotic DSBs. Quantification of DSB levels appear at the bottom of each blot. SPM, sporulation media.

(D) Pie chart representation of Rad51 peak loss in H4K44R (78% loss, 330 of 423).

(E) Boxplot representation of Rad51 enrichment (relative to input) at Rad51 peaks. Rad51 reduction in H4K44R is significant at the 330 lost peaks (Wilcoxon test: $^{**}p < 2.2 \times 10^{-16}$), while there is no significant change in the set of 93 retained peaks ($p = 0.1702$). The area under the curve over the Rad51 peaks is used to estimate the p value.

(F) UCSC track showing decreased Rad51 at DSB hotspots in H4K44R relative to WT. Black bars represent DSB hotspots (Pan et al., 2011).

See also Figure S2 and Table S1.

the resulting tetrad spores in the H4K44R mutant were inviable (Figure 1E). H4K44R spore inviability suggests a defect in chromosome segregation (Keeney, 2001), implicating that meiotic recombination may be compromised in H4K44R.

H4K44ac Is Important for Meiotic Recombination

H4K44ac enrichment during meiosis (Figure 1C) and the extremely low spore viability in H4K44R (Figure 1E) led us to focus on the role of H4K44ac during meiotic recombination. First, we examined the effect of H4K44R in a random spore analysis assay measuring recombination frequency between heteroalleles of the *HIS4* locus during meiosis. H4K44R displayed a significant decrease in meiotic recombination events at *HIS4*, compared to less than 50% of WT H4 recombination (Figure 2A, bottom panels).

We next analyzed whether DSB formation was affected in H4K44R. We directly analyzed meiotic DSB formation at two well-studied DSB hotspots, *FRS2-GAT1* and *BUD23-ARE1* (Figures 2B and 2C) (Acquaviva et al., 2013; Yamashita et al., 2004). Meiotic DSBs at each hotspot were reduced in H4K44R compared to WT, determined by Southern blot using hotspot probes (Figures 2B and 2C). We also performed pulsed-field gel electrophoresis (PFGE) to detect genome-wide meiotic DSBs (EtBr stain) (Figure S2A) and DSBs on chromosome 3 (Southern blot using probe to *CHA1*) (Figures S2B and S2C). These analyses confirmed that fewer DSBs form in H4K44R compared to WT.

To advance this observation and to compare genome-wide DSB formation and repair, we performed Rad51 chromatin immunoprecipitation sequencing (ChIP-seq) (Smagulova et al., 2011). Recombinases Rad51 and Dmc1 form nucleoprotein filaments on single-stranded DNA at processed DSBs and are required for repair (Neale and Keeney, 2006); thus, we used Rad51 enrichment as an independent marker for DSB formation and repair. Rad51 ChIP-seq data were highly reproducible between biological replicates (Figure S2D) and showed reproducible reduction of Rad51 enrichment in H4K44R compared to WT (Figures 2F, S2E, and S2F).

To more specifically determine differences in Rad51 peaks between WT and H4K44R, we identified 423 Rad51 peaks in WT (Table S1) using model-based analysis of ChIP-seq (see Experimental Procedures). Of these, 330 (78%) were undetected in H4K44R, with 93 Rad51 peaks maintained in H4K44R (Figures 2D and 2E), indicating significant Rad51 reduction in the mutant. Consistent with Rad51 enrichment at DSBs (Neale and Keeney, 2006), Rad51 peaks were highly correlated with Spo11 DSB hotspots (WT, $p = 0.018$; H4K44R, $p < 0.001$) (Figure S2F). The 153 Rad51 peaks were identified in H4K44R only; however, Rad51 enrichment at these peaks is lower than at Rad51 peaks in only WT or shared between WT and H4K44R (Figures S2G and S2H). Thus, H4K44R-only Rad51 peaks may be an artifact of

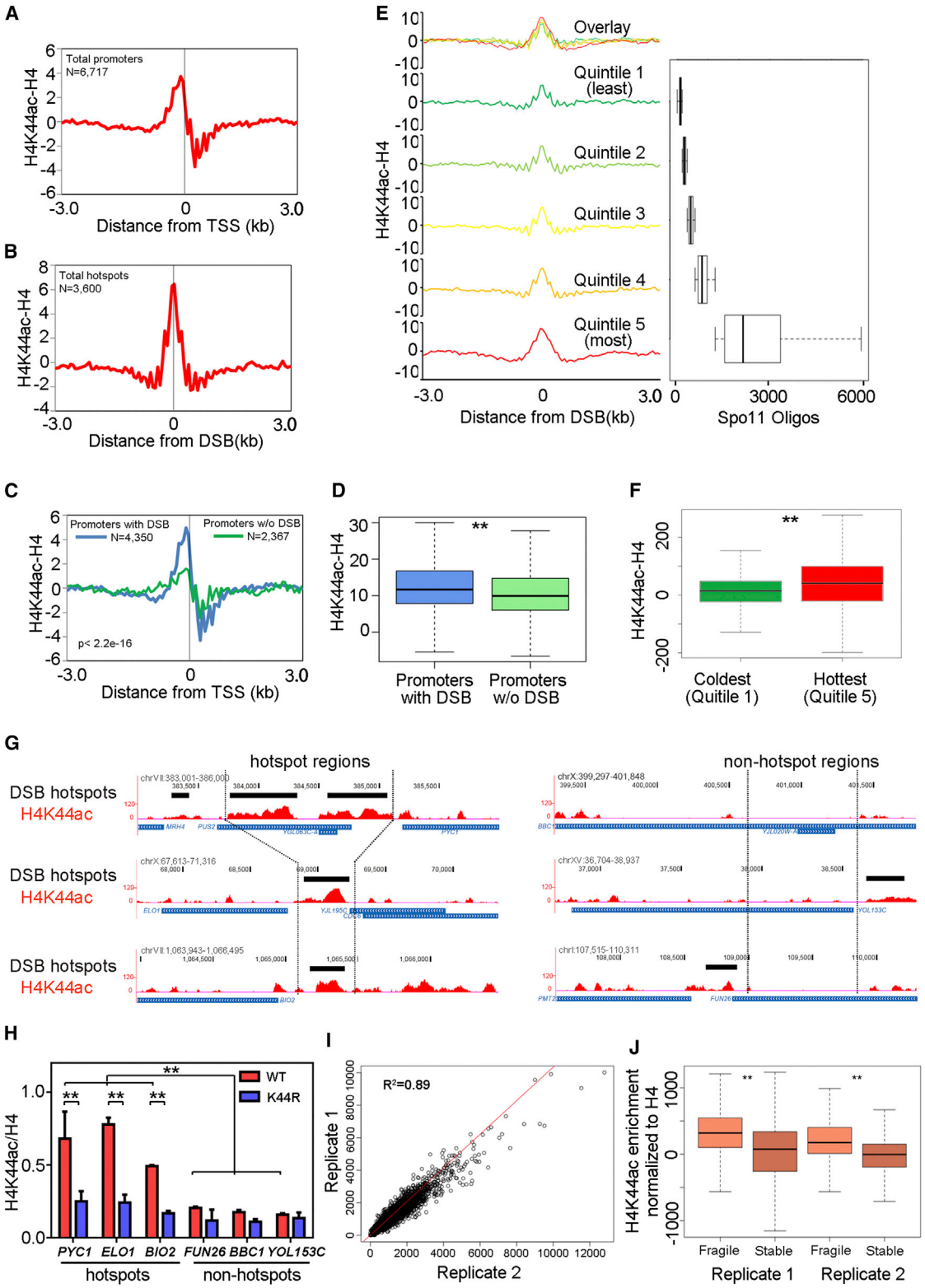

Figure 3. H4K44ac Is Enriched at Recombination Hotspots

(A) Metaplot representation of the distribution of H4K44ac around all TSSs in *S. cerevisiae*.

(B) Metaplot representation of the distribution of H4K44ac around meiotic recombination hotspots.

(legend continued on next page)

MACS, due to the low Rad51 signal in H4K44R (Figure S2E), or they may mark regions of transient Rad51 binding in H4K44R. The overall observation of significant Rad51 reduction in H4K44R, taken together with the Southern blot and PFGE analysis, indicate that DSB formation and meiotic recombination are reduced in H4K44R and suggest that H4K44ac is required for normal levels of DSB formation.

H4K44ac Marks Meiotic DSB Hotspots

Based on our observations, we postulated that H4K44ac may be specifically enriched at DSB hotspots. To test this, we performed H4K44ac ChIP-seq in WT meiotic cells at peak DSB formation (4 hr) to determine the genomic distribution of the modification. Strikingly, H4K44ac mapped preferentially to intergenic regions containing promoters (Figure 3A), indicating a possible association with DSB hotspots, which generally are formed in intergenic promoters (Pan et al., 2011). To address this directly, we examined the H4K44ac enrichment at DSBs, using a recent high-resolution genome-wide DSB map (Pan et al., 2011). H4K44ac showed significantly strong enrichment at hotspot centers (Figure 3B, $p < 0.01$). H4K44ac enrichment at DSB hotspots is partly because of the co-occurrence of DSBs at promoters. To determine whether H4K44ac is more specific to the promoters with DSB hotspots, we divided promoters into two classes: those overlapping (4,350) or not overlapping (2,367) DSB hotspots (defined as the region 400 bp upstream from transcription start sites, or TSSs) (Tischfield and Keeney, 2012). On average, promoters with hotspots showed obvious and significantly higher H4K44ac enrichment than non-hotspot promoters (Figures 3C and 3D). This observation was validated by ChIP-qPCR, randomly examining two promoters from each class (Figure S3A).

To further determine a quantitative relationship between H4K44ac levels and DSBs, we subdivided promoter hotspots into five quintiles based on Spo11 enrichment (Figure 3E, right panel). Average H4K44ac enrichment profiles (Figure 3E, left panel) show that H4K44ac correlates to DSB "hotness"; we observe higher H4K44ac enrichment in the hottest DSB quintile (most Spo11) relative to the coldest (least Spo11) (Figure 3F). The difference in H4K44ac enrichment across quintiles is modest relative to the extreme difference in Spo11 enrichment per quintile (~20-fold difference in medians) (Figure 3E, right panel); correlation between H4K44ac levels and DSB strength is small ($R^2 = 0.003$) when measuring H4K44ac enrichment at individual promoter hotspots (Figure S3B). Thus, our results indicate that H4K44ac is a histone modification that occurs specifically at DSB hotspots. However, enrichment of the modification alone is unlikely to be predictive of levels of DSB formation, as is the case for H3K4me3 (Tischfield and Keeney, 2012).

We further determined whether non-modifiable H4K44R has an impact on other important meiotic histone modifications, thus acting indirectly through other modifications. We analyzed H3K4me3, important for meiotic recombination and enriched at DSB hotspots (Acquaviva et al., 2013; Borde et al., 2009; Sollier et al., 2004; Sommermeyer et al., 2013), and H3K56ac associated with meiosis (Figure 1C) (Govin et al., 2010a; Recht et al., 2006). We performed western blots to examine levels of H3K4me3 and H3K56ac during sporulation in WT and H4K44R, and we found no obvious change in timing and relative abundance of each modification (Figure S3C). We also investigated genome-wide distributions of H3K4me3 and H3K56ac using ChIP-seq, following the same time profiling as in the H4K44ac studies. We observed a modest decrease (less than 20%) of either H3K4me3 or H3K56ac enrichment at gene promoters or DSB hotspots in H4K44R compared to WT (Figures S3D–S3H), which may be due to a secondary effect of abnormal DSB formation in H4K44R cells. The H3K4me3 and H3K56ac analyses indicate that H4K44ac appears to function in meiotic recombination independent of a known chromatin pathway.

H4K44ac enrichment perplexingly appears almost directly over the DSB hotspots, which are previously defined promoter nucleosome-depleted regions (Pan et al., 2011). To address this possible paradox, we first validated the ChIP-seq data and confirmed the specificity of the H4K44ac antibody for ChIP. We randomly examined by ChIP-qPCR three DSB hotspots: *BIO2*, *ELO1*, and *PYC1* (track views shown in Figure 3G), which are within gene promoters. As expected based on ChIP-seq results, H4K44ac is enriched at these DSB promoters relative to control loci within gene bodies. H4K44ac enrichment was greatly reduced in H4K44R mutants at all measured loci (Figure 3H). To further validate H4K44ac ChIP-seq enrichment, we performed an independent biological H4K44ac ChIP-seq replicate, which yielded consistent results (Figure 3I).

(C) Metaplot representation of the distribution of H4K44ac around TSSs with a DSB hotspot (blue, n = 4,350) versus those without (green, n = 2,367). The maximum value for the H4K44ac profile for each gene between 500 bp upstream and TSSs was calculated for the p value.

(D) Boxplot representation of the distribution of H4K44ac enrichment at a 500 bp window upstream of TSSs from each group in (C). H4K44ac enrichment is significantly different at TSSs with a DSB hotspot versus those without (Wilcoxon test: $^{**}p < 2.2 \times 10^{-16}$). The p value was estimated as in (C).

(E) H4K44ac enrichment for promoter hotspots divided into quintiles by Spo11 strength. Boxplots (right) show the distribution of Spo11 within each quintile.

(F) Boxplot representation of H4K44ac enrichment at each quintile from (E). H4K44ac enrichment is significantly different at the lowest and highest Spo11 quintiles (Wilcoxon test: $^{**}p = 1.5 \times 10^{-9}$). The p value was estimated from areas under the curve of 400 bp around the Spo11 peak centers.

(G) UCSC track showing the distribution of H4K44ac enrichment at selected DSB hotspots (left) and control regions (right). Black bars represent DSB hotspots (Pan et al., 2011).

(H) ChIP-qPCR validation of H4K44ac enrichment at DSB hotpots. PCR primers are designed within the regions marked in (C). Mean ± SEM of three independent experiments. The difference is statistically significant: $^{**}p < 0.01$.

(I) Scatter plot of H4K44ac enrichment intensities over 3,600 Spo11 DSBs between two independent H4K44ac ChIP-seq experiments, showing a high degree of correlation ($R^2 = 0.89$).

(J) Boxplot representation of H4K44ac over 3,341 fragile nucleosomes and 58,673 stable nucleosomes (Xi et al., 2011), showing enrichment at fragile nucleosome sites. H4K44ac enrichment is significantly different between fragile and stable nucleosomes (Wilcoxon test: $^{**}p < 1 \times 10^{-16}$).

See also Figure S3.

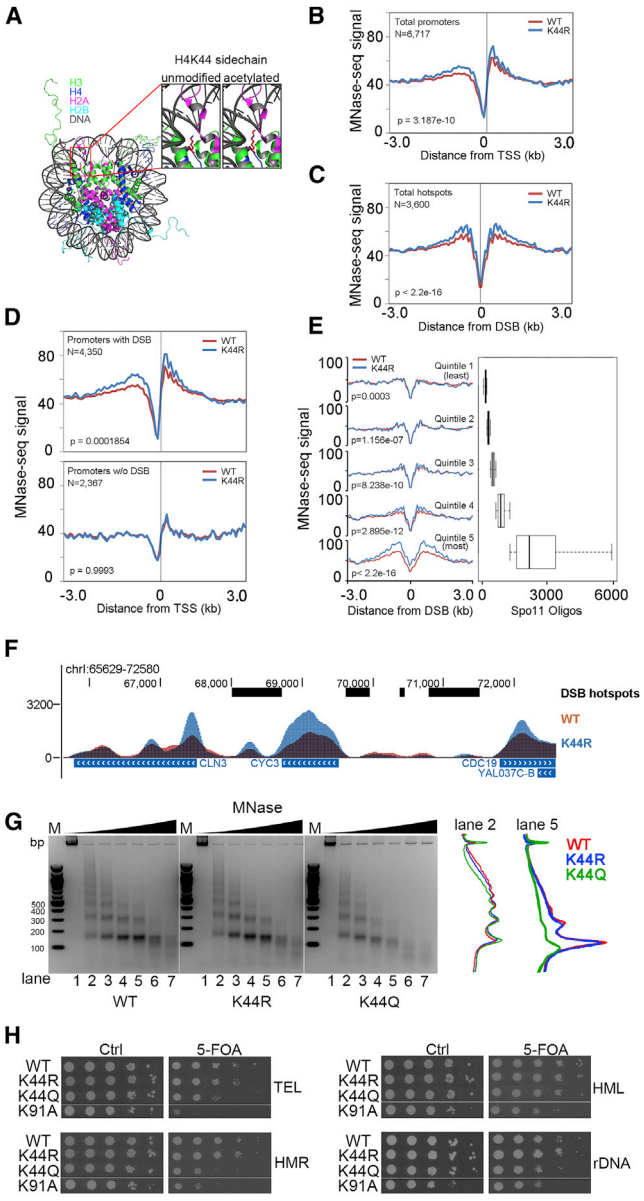

Figure 4. H4K44ac Contributes to the Chromatin Openness

(A) Nucleosome image of the full histone octamer. The side chain containing H4K44 is shown in both unmodified and acetylated states (PyMOL, PDB: 1ID3).

(B and C) Nucleosome occupancy profiles of WT (red) and H4K44R (blue) at peri-TSS regions (B) and DSB hotspots (C), indicating significantly increased occupancy in H4K44R. p values were estimated from the maximum value 500 bp downstream of TSSs and 500 bp around Spo11 hotspots for (B) and (C), respectively.

(D) Nucleosome occupancy profiles of WT (red) and H4K44R (blue) at TSSs with a DSB hotspot (top) versus those without (bottom). Nucleosome occupancy is significantly increased in H4K44R at promoters with DSBs only. p values were estimated as in (B).

(E) Nucleosome occupancy profiles of WT (red) and H4K44R (blue) at Spo11 quintiles. Boxplots (right) show distribution of Spo11 enrichment within quintiles. p values were estimated as in (C).

(F) Example overlaid the MNase-seq track of WT (orange) and H4K44R (blue), showing increased nucleosome occupancy of H4K44R (blue over black curve) around DSB hotspots. Black bars represent DSB hotspots; the track was smoothed with 15 pixels.

(G) MNase-accessibility assay indicating increased chromatin accessibility in H4K44Q (right) compared to WT (left) and H4K44R (middle). A representative of three biological replicates is shown. The quantitative densitometric analysis of the indicated lanes is shown on the right.

(H) Spot dilutions of WT, H4K44R, and H4K44Q strains carrying *URA3* at the silent mating locus HMR indicate a growth defect in H4K44Q on 5-FOA (right) compared to YPD control (left). A representative result of two biological replicates is shown. The H4K91A mutant (Ye et al., 2005) is a positive control. See also Figure S4.

We then considered how H4K44ac enrichment occurs in regions expected to be nucleosome depleted. Previous reports have described highly sensitive nucleosomes located within nucleosome-depleted regions, suggesting that these regions are not devoid of nucleosomes but are associated with "fragile nucleosomes" (Weiner et al., 2010; Xi et al., 2011). We measured H4K44ac enrichment in regions of fragile and stable nucleosomes and observed significantly higher H4K44ac at fragile versus stable nucleosomes in both biological replicate ChIP-seq datasets (Figure 3J). This observation suggests that H4K44ac may be associated with nucleosome fragility at certain sites and may contribute to nucleosome instability or weak histone-and-DNA interaction, as investigated later.

H4K44ac Influences Chromatin Structure

Lateral surface histone modifications generally influence nucleosome stability (Tropberger and Schneider, 2013). H4K44 exists at the L1 loop linking α helix1 and α helix2 of histone H4, located close to the DNA entry-exit region of the nucleosome (Figure 4A), and thus could contribute to chromatin organization. Meiotic micrococcal nuclease (MNase) digestion analysis has shown that some recombination hotspots exhibit an increase in MNase accessibility prior to the appearance of meiotic DSBs (Ohta et al., 1994). Therefore, we tested whether H4K44ac regulates chromatin accessibility during meiosis using meiotic micrococcal nuclease sequencing (MNase-seq) to determine nucleosome positioning in WT and H4K44R during peak meiotic DSB formation (4 hr) compared to vegetative growth (YPD media) and presporulation (0 hr; YPA media). Overall nucleosome occupancy was elevated in H4K44R compared to WT in the regions surrounding all TSSs (Figure 4B) and DSB hotspots at 4 hr (Figure 4C). No detectable nucleosome occupancy changes were observed between H4K44R and WT in YPD or at 0 hr (Figures S4A–S4D), suggesting that H4K44ac promotes chromatin accessibility when meiotic recombination is initiated. The increased nucleosome occupancy observed at 4 hr in H4K44R is more clearly visualized in overlaid WT and H4K44R tracks at representative DSB hotspots (Figure 4F).

We further investigated the correlation between nucleosomal occupancy changes and DSB hotspots between H4K44R and WT. As with the H4K44ac analyses (Figures 3C and 3E), we divided all promoters into those with and those without hotspots and then divided all hotspot promoters into quintiles of DSB strength. We observed that nucleosome occupancy in H4K44R at 4 hr is specifically increased at promoters with DSB hotspots (Figure 4D) and that increased nucleosome occupancy

correlates with DSB strength (Figure 4E). Taken together, these observations support a function for H4K44ac in facilitating or maintaining chromatin accessibility at DSB hotspots in meiosis.

In contrast to H4K44R, we speculated that the H4K44Q constitutive acetylation mimic mutant should exhibit decreased nucleosome density. H4K44Q cells displayed severe growth limitation under pre-sporulation acetate conditions and failed to initiate pre-meiotic DNA replication or enter meiosis (Figures S4E–S4G; compare to H4K44R). Thus, we could not address the consequence of H4K44Q during meiosis and sporulation; the failure of meiotic induction may result from a deleterious effect of mimicking constitutive acetylation. As an alternative, we characterized H4K44Q in logarithmically growing cells. First, we examined nucleosome accessibility by MNase digestion in H4K44Q, H4K44R, and WT strains. Equal numbers of nuclei from cycling cells were treated with an increasing concentration of MNase, and the resulting digestion profiles were compared between strains. H4K44Q cells showed extensive digestion compared to WT and H4K44R cells (Figure 4G, lane 5), indicating a more accessible chromatin structure in the constitutive acetylation-like state at H4K44.

Finally, we tested functional effects of H4K44 substitutions using a classic heterochromatin silencing assay (van Leeuwen et al., 2002), reasoning that increased accessibility would de-silence a reporter placed in normally closed chromatin. We examined effects of H4K44R and H4K44Q substitutions on expression of *URA3* integrated (1) near the left telomere of chromosome VII (*Tel VII-L*), (2) within the silent *MAT* loci, and (3) within the *rDNA* repeats. Expression of *URA3* causes conversion of 5-fluoroorotic acid (5-FOA) in the growth medium into toxic 5-fluorouracil. Based on our other observations, we predicted that H4K44Q would display defective silencing, and de-silencing occurred in H4K44Q at *Tel VII-L*, *HMR* (the effect was subtle at *HML*), and rDNA loci (Figure 4H). Silencing was not affected in the H4K44R mutation (Figure 4H), as expected because acetylation is not likely occurring at silenced heterochromatin (Richards and Elgin, 2002) and because H4K44ac is not enriched in mitotic cells (Figures 1B and S1C). For comparison, we tested H4K91A, which has a strong silencing phenotype and is important for chromatin structure (Ye et al., 2005), and we found similar silencing defects between H4K44Q and H4K91A (Figure 4H). Thus, constitutive acetylation mimic at H4K44 results in increased MNase accessibility, compromised heterochromatin maintenance, and failure to induce sporulation. Together with the preceding data, these results underscore an important role for acetylation at H4K44 in regulating chromatin accessibility during meiosis.

DISCUSSION

In this study, we identified and characterized the function of H4K44ac, a previously undiscovered histone modification enriched in pre-meiotic and meiotic yeast and located on the nucleosomal lateral surface adjacent to the DNA backbone. Substitution of this residue to non-modifiable H4K44R confers reduction in meiotic recombination rate (Figure 2A) and DSB formation (Figures 2B, 2C, and S2A–S2C), and it manifests in severe spore inviability (Figure 1E). In addition, genome-wide H4K44ac enrichment shows high correlation with DSB hotspots (Figures 3A–3F) and with locations of fragile nucleosomes (Figure 3J). H4K44R mutants show specific increased nucleosome occupancy around DSB hotspots during meiosis (Figures 4B–4E and S4A–S4D); in contrast, H4K44Q mutants show increased MNase accessibility during mitosis (Figure 4G). Together, these data support a model in which acetylation at H4K44 on the histone globular core results in increased chromatin accessibility during meiosis.

This role is distinct from our previous study of post-meiotic histone H4 tail acetylation in chromatin compaction (Govin et al., 2010a). H4K44ac peaks during meiotic DSB formation and repair, which may be favorable for chromatin accessibility of key DSB-associated complexes to initiate and complete meiotic recombination. We propose that H4K44ac may play an important role in increasing chromatin accessibility via nucleosome-DNA destabilization, as has been shown for H3K64ac and H3K122ac on the histone H3 globular domain (Di Cerbo et al., 2014; Tropberger et al., 2013), whereas H4K16ac on the histone H4 tail inhibits inter-fiber interaction (Shogren-Knaak et al., 2006).

We observed preferential enrichment of H4K44ac at gene promoters with DSB hotspots compared with at those without hotspots and an increase of nucleosome occupancy around hotspot promoters in H4K44R at 4 hr rather than in YPD or 0 hr, in support of a direct role of H4K44ac in meiosis. However, H4K44ac alone is an insufficient indicator of the quantitative levels of DSB activity (Figure S3B). Likewise, the overall nucleosome occupancy increase in H4K44R, while significant, is not as high as may be expected given the significant reduction in DSB formation compared to WT. This observation is likely due to the average effect of analyzing nucleosome occupancy at hotspots over the cell population, obscuring larger changes that may be occurring in individual H4K44R mutant cells. There are thousands of Spo11 binding sites across the yeast genome, but only an estimated ~160 actual DSBs occur per meiotic cell (Pan et al., 2011). We speculate that general increased chromatin accessibility at 4 hr in meiosis, mediated in part by acetylation at H4K44, is likely a prerequisite for DSB formation, and local chromatin structural changes at individual hotspots may vary within a population due to cell-to-cell variability.

While our observations highlight a role for H4K44ac during meiosis, H4K44ac is not meiosis specific but is observed in pre-meiosis (Figures 1B and 1C). The reduction between 0 and 4 hr during meiosis is possibly caused by passive loss via DNA replication during the meiotic S phase. H4K44ac is observed only after switching the yeast into pre-sporulation acetate medium, indicative of a potential response from the absence of normal glucose growth conditions. H3K4me3, which is important for meiotic DSB formation, is present in exponentially growing cells and is maintained at all sporulation stages (Figure 1C) (Borde et al., 2009), and the switch between the vegetative and the meiotic functions may be due to its binding factor Spp1 (Acquaviva et al., 2013; Sommermeyer et al., 2013). Thus, we speculate that H4K44ac may be associated with pre-meiotic transcriptional changes upon the switch into acetate medium. Considering that we observe no difference in nucleosome occupancy in H4K44R at 0 hr when H4K44ac is enriched (Figures S4C

and S4D), another possibility is that the enzyme for H4K44ac is activated upon pre-meiotic induction (described later) but an additional Spp1-like factor may regulate the function of this modification.

Although K-to-R/Q substitution is a widely used strategy to characterize the function of lysine acetylation, these mutants may still cause unrelated phenotypes from differences in the amino acid structures. To overcome this limitation, it is important to determine the enzyme that acetylates H4K44 in meiosis to further characterize the modification. Based on previous yeast meiotic transcriptome data (Primig et al., 2000), we surveyed expression of known histone acetyltransferases (Gcn5, Hat1, Hat2, Hpa1, Hpa2, Hpa3, Sas2, Sas3, Sas4, Sas5, Rtt109, Spt10, and Esa1). We identified only Rtt109 as having a similar expression pattern to that of H4K44ac during meiosis. However, Rtt109 does not show enzymatic activity on histone H4 (Driscoll et al., 2007; Han et al., 2007); thus, further investigation is required to identify the specific enzyme for H4K44ac.

Our observations provide additional insight into the direct role of histone modifications on meiotic recombination and support previous studies of chromatin openness at DSB hotspots (Pan et al., 2011). Furthermore, H4K44ac occurs near the DNA entry-exit point of the nucleosome and may play a role in nucleosome stability, supported by H4K44ac enrichment at fragile nucleosomes (Figure 3J). The other known acetylated lysine residues located on the lateral surface, H3K64 and H3K122, affect nucleosome dynamics and regulate gene transcription (Di Cerbo et al., 2014; Tropberger et al., 2013). These functions appear to be distinct from H4K44ac, which contributes to normal programmed recombination in sporulation. Hence, acetylation at different sites on the nucleosome lateral surface may exhibit specificity in molecular function based on location. It is of great interest to further characterize the mechanisms of these modifications in regulating distinct biological processes.

EXPERIMENTAL PROCEDURES

Yeast Strains

The genotypes of all yeast strains and applications are listed in Table S2.

ChIP and ChIP-Seq Analysis

ChIP assays were performed as described (Govin et al., 2010b). Sequences of primers used for ChIP-qPCR can be found in Table S3. ChIP-seq libraries were prepared with the NEBNext ChIP-seq Library Prep Reagent Set for Illumina and were single-end sequenced with Illumina HiSeq 2000 or NextSeq 500 platforms.

MNase Digestion and Preparation of Mononucleosomal DNA for Sequencing

MNase digestion assays were performed as described previously (Rando, 2010). Mononucleosomal DNA was isolated and end repaired for library preparation; libraries were constructed with the NEBNext Ultra DNA Library Prep Kit for Illumina and single-end sequenced using Illumina HiSeq 2000 or NextSeq 500 platforms.

Raw sequenced data were produced via Illumina sequencing (Hi-Seq for WT and H4K44R MNase-seq, histone post-translational modification, and H4 data; NextSeq 2000 for all others). ChIP-seq and MNase-seq data were aligned to the yeast sacCer2 assembly using bowtie v.1.0 (parameters –m 1 and –best). All sequencing data are supplied on GEO: GSE59005. Detailed experimental methods and data analyses are provided in the Supplemental Experimental Procedures.

ACCESSION NUMBERS

The accession number for the sequencing data reported in this paper is GEO: GSE59005.

SUPPLEMENTAL INFORMATION

Supplemental Information includes Supplemental Experimental Procedures, four figures, and three tables and can be found with this article online at http://dx.doi.org/10.1016/j.celrep.2015.10.070.

ACKNOWLEDGMENTS

We thank the IDOM Functional Genomics Core Sequencing Facility for ChIP-seq and MNase-seq. This work was supported by NIH grants GM055360 and U54-HD068157 awarded to S.L.B.

Received: November 21, 2014
Revised: August 10, 2015
Accepted: October 24, 2015
Published: November 25, 2015

REFERENCES

Acquaviva, L., Székvölgyi, L., Dichtl, B., Dichtl, B.S., de La Roche Saint André, C., Nicolas, A., and Géli, V. (2013). The COMPASS subunit Spp1 links histone methylation to initiation of meiotic recombination. Science *339*, 215–218.

Bell, O., Tiwari, V.K., Thomä, N.H., and Schübeler, D. (2011). Determinants and dynamics of genome accessibility. Nat. Rev. Genet. *12*, 554–564.

Borde, V., Robine, N., Lin, W., Bonfils, S., Géli, V., and Nicolas, A. (2009). Histone H3 lysine 4 trimethylation marks meiotic recombination initiation sites. EMBO J. *28*, 99–111.

Cosgrove, M.S., Boeke, J.D., and Wolberger, C. (2004). Regulated nucleosome mobility and the histone code. Nat. Struct. Mol. Biol. *11*, 1037–1043.

Di Cerbo, V., Mohn, F., Ryan, D.P., Montellier, E., Kacem, S., Tropberger, P., Kallis, E., Holzner, M., Hoerner, L., Feldmann, A., et al. (2014). Acetylation of histone H3 at lysine 64 regulates nucleosome dynamics and facilitates transcription. eLife *3*, e01632.

Driscoll, R., Hudson, A., and Jackson, S.P. (2007). Yeast Rtt109 promotes genome stability by acetylating histone H3 on lysine 56. Science *315*, 649–652.

Govin, J., Dorsey, J., Gaucher, J., Rousseaux, S., Khochbin, S., and Berger, S.L. (2010a). Systematic screen reveals new functional dynamics of histones H3 and H4 during gametogenesis. Genes Dev. *24*, 1772–1786.

Govin, J., Schug, J., Krishnamoorthy, T., Dorsey, J., Khochbin, S., and Berger, S.L. (2010b). Genome-wide mapping of histone H4 serine-1 phosphorylation during sporulation in *Saccharomyces cerevisiae*. Nucleic Acids Res. *38*, 4599–4606.

Han, J., Zhou, H., Horazdovsky, B., Zhang, K., Xu, R.M., and Zhang, Z. (2007). Rtt109 acetylates histone H3 lysine 56 and functions in DNA replication. Science *315*, 653–655.

Hunter, N. (2007). Meiotic recombination. In Molecular Genetics of Recombination, A. Aguilera and R. Rothstein, eds. (Springer Berlin Heidelberg), pp. 381–442.

Keeney, S. (2001). Mechanism and control of meiotic recombination initiation. Curr. Top. Dev. Biol. *52*, 1–53.

Keeney, S. (2008). Spo11 and the formation of DNA double-strand breaks in meiosis. Genome Dyn. Stab. *2*, 81–123.

Krishnamoorthy, T., Chen, X., Govin, J., Cheung, W.L., Dorsey, J., Schindler, K., Winter, E., Allis, C.D., Guacci, V., Khochbin, S., et al. (2006). Phosphorylation of histone H4 Ser1 regulates sporulation in yeast and is conserved in fly and mouse spermatogenesis. Genes Dev. *20*, 2580–2592.

Musselman, C.A., Lalonde, M.E., Côté, J., and Kutateladze, T.G. (2012). Perceiving the epigenetic landscape through histone readers. Nat. Struct. Mol. Biol. *19*, 1218–1227.

Neale, M.J., and Keeney, S. (2006). Clarifying the mechanics of DNA strand exchange in meiotic recombination. Nature *442*, 153–158.

Ohta, K., Shibata, T., and Nicolas, A. (1994). Changes in chromatin structure at recombination initiation sites during yeast meiosis. EMBO J. *13*, 5754–5763.

Pan, J., Sasaki, M., Kniewel, R., Murakami, H., Blitzblau, H.G., Tischfield, S.E., Zhu, X., Neale, M.J., Jasin, M., Socci, N.D., et al. (2011). A hierarchical combination of factors shapes the genome-wide topography of yeast meiotic recombination initiation. Cell *144*, 719–731.

Primig, M., Williams, R.M., Winzeler, E.A., Tevzadze, G.G., Conway, A.R., Hwang, S.Y., Davis, R.W., and Esposito, R.E. (2000). The core meiotic transcriptome in budding yeasts. Nat. Genet. *26*, 415–423.

Rando, O.J. (2010). Genome-wide mapping of nucleosomes in yeast. Methods Enzymol. *470*, 105–118.

Recht, J., Tsubota, T., Tanny, J.C., Diaz, R.L., Berger, J.M., Zhang, X., Garcia, B.A., Shabanowitz, J., Burlingame, A.L., Hunt, D.F., et al. (2006). Histone chaperone Asf1 is required for histone H3 lysine 56 acetylation, a modification associated with S phase in mitosis and meiosis. Proc. Natl. Acad. Sci. USA *103*, 6988–6993.

Richards, E.J., and Elgin, S.C. (2002). Epigenetic codes for heterochromatin formation and silencing: rounding up the usual suspects. Cell *108*, 489–500.

Shogren-Knaak, M., Ishii, H., Sun, J.M., Pazin, M.J., Davie, J.R., and Peterson, C.L. (2006). Histone H4-K16 acetylation controls chromatin structure and protein interactions. Science *311*, 844–847.

Smagulova, F., Gregoretti, I.V., Brick, K., Khil, P., Camerini-Otero, R.D., and Petukhova, G.V. (2011). Genome-wide analysis reveals novel molecular features of mouse recombination hotspots. Nature *472*, 375–378.

Sollier, J., Lin, W., Soustelle, C., Suhre, K., Nicolas, A., Géli, V., and de La Roche Saint-André, C. (2004). Set1 is required for meiotic S-phase onset, double-strand break formation and middle gene expression. EMBO J. *23*, 1957–1967.

Sommermeyer, V., Béneut, C., Chaplais, E., Serrentino, M.E., and Borde, V. (2013). Spp1, a member of the Set1 Complex, promotes meiotic DSB formation in promoters by tethering histone H3K4 methylation sites to chromosome axes. Mol. Cell *49*, 43–54.

Tischfield, S.E., and Keeney, S. (2012). Scale matters: the spatial correlation of yeast meiotic DNA breaks with histone H3 trimethylation is driven largely by independent colocalization at promoters. Cell Cycle *11*, 1496–1503.

Tropberger, P., and Schneider, R. (2013). Scratching the (lateral) surface of chromatin regulation by histone modifications. Nat. Struct. Mol. Biol. *20*, 657–661.

Tropberger, P., Pott, S., Keller, C., Kamieniarz-Gdula, K., Caron, M., Richter, F., Li, G., Mittler, G., Liu, E.T., Bühler, M., et al. (2013). Regulation of transcription through acetylation of H3K122 on the lateral surface of the histone octamer. Cell *152*, 859–872.

van Leeuwen, F., Gafken, P.R., and Gottschling, D.E. (2002). Dot1p modulates silencing in yeast by methylation of the nucleosome core. Cell *109*, 745–756.

Weiner, A., Hughes, A., Yassour, M., Rando, O.J., and Friedman, N. (2010). High-resolution nucleosome mapping reveals transcription-dependent promoter packaging. Genome Res. *20*, 90–100.

Wu, T.C., and Lichten, M. (1994). Meiosis-induced double-strand break sites determined by yeast chromatin structure. Science *263*, 515–518.

Wysocka, J., Swigut, T., Xiao, H., Milne, T.A., Kwon, S.Y., Landry, J., Kauer, M., Tackett, A.J., Chait, B.T., Badenhorst, P., et al. (2006). A PHD finger of NURF couples histone H3 lysine 4 trimethylation with chromatin remodelling. Nature *442*, 86–90.

Xi, Y., Yao, J., Chen, R., Li, W., and He, X. (2011). Nucleosome fragility reveals novel functional states of chromatin and poises genes for activation. Genome Res. *21*, 718–724.

Yamashita, K., Shinohara, M., and Shinohara, A. (2004). Rad6-Bre1-mediated histone H2B ubiquitylation modulates the formation of double-strand breaks during meiosis. Proc. Natl. Acad. Sci. USA *101*, 11380–11385.

Ye, J., Ai, X., Eugeni, E.E., Zhang, L., Carpenter, L.R., Jelinek, M.A., Freitas, M.A., and Parthun, M.R. (2005). Histone H4 lysine 91 acetylation a core domain modification associated with chromatin assembly. Mol. Cell *18*, 123–130.

Zhang, L., Ma, H., and Pugh, B.F. (2011). Stable and dynamic nucleosome states during a meiotic developmental process. Genome Res. *21*, 875–884.